

Measurement of the band gap of $\text{Ge}_x\text{Si}_{1-x}/\text{Si}$ strained-layer heterostructures

D. V. Lang, R. People, J. C. Bean, and A. M. Sergent
AT&T Bell Laboratories, Murray Hill, New Jersey 07974

(Received 9 September 1985; accepted for publication 14 October 1985)

We have used photocurrent spectroscopy to measure the optical absorption spectra of coherently strained layers of $\text{Ge}_x\text{Si}_{1-x}$ grown on $\langle 001 \rangle$ Si by molecular beam epitaxy. A dramatic lowering of the indirect band gap, relative to that of unstrained bulk Ge-Si alloys, is observed. Our results for $0 < x < 0.7$ are in remarkably good agreement with recent calculations of the effects of misfit strain on the band edges of coherently strained Ge-Si heterostructures. At $x = 0.6$, the gap is lower than that of pure Ge.

It is well known that the fundamental (indirect) band gap of bulk $\text{Ge}_x\text{Si}_{1-x}$ alloys spans the 1.30–1.55- μm range.¹ This fact makes such alloys extremely attractive for applications involving long wavelength integrated optoelectronics on Si. It has been demonstrated recently that $\text{Ge}_x\text{Si}_{1-x}/\text{Si}$ heterostructures having good electrical quality² can be fabricated on Si substrates if the alloy layers are kept sufficiently thin.³ Furthermore, high quality Ge-Si/Si strained layer superlattices (SLS's) can be grown free of misfit dislocations³⁻⁵; the lattice mismatch in these structures being accommodated by coherent layer strains.⁶ The strains present in SLS's may dramatically alter the optical and electronic properties of these structures, in comparison to the bulk constituents.⁷ Recent calculations of the effects of misfit strain on the band edges of coherently strained Ge-Si/Si heterostructures predict a dramatic lowering of the fundamental band gap of the alloy layers.⁸ In this letter, we present the first measurements of the band gap of coherently strained $\text{Ge}_x\text{Si}_{1-x}/\text{Si}$ heterostructures. Photocurrent spectroscopy has been used to measure the optical absorption spectra of coherently strained multilayers having $0 < x < 0.7$. These results are in remarkably good agreement with the earlier predictions.⁸

The samples were Ge-Si/Si strained-layer superlattices (SLS's) grown in a p - i - n diode configuration. The Si substrate was n type 0.5–3.0 Ω cm (phosphorus). The molecular beam epitaxy (MBE) growth consisted of an As-doped n layer 0.5 μm thick with a net donor concentration of $5 \times 10^{16} \text{ cm}^{-3}$. The undoped Ge-Si SLS formed the i layer of the diode. It consisted of 20 pairs of layers of 250 \AA Si and 75 \AA Ge-Si alloy for a total thickness of 0.65 μm . The top p layer was doped with $1 \times 10^{17} \text{ cm}^{-3}$ boron and was 1 μm thick. The Ge content of the Ge-Si layers of the SLS varied from 0 to 70 mol %. The photocurrent measurements were made on cleaved rectangles roughly 1 mm on a side. Ohmic contacts were made to the back of these pieces and to a small spot on the p layer with an In-Ga mixture using a slight mechanical abrasion. This procedure was useful in avoiding unnecessary processing of the sample while maintaining a transparent front surface.

The photocurrent measurements were made in a standard way using a grating monochromator in the range 0.9–2.5 μm with either GaAs, Si, or Ge filters and lock-in detection at 100 Hz. A portion of the light incident on the sample was deflected to a calibrated PbS detector so that the sample

photocurrent could be normalized to the incident intensity. The absorption coefficient α is proportional to the photocurrent per incident photon when the absorbing layer thickness is much less than α^{-1} . This is true in our case. All measurements were made at zero bias in a dewar with the sample mounted just above liquid nitrogen at a temperature of roughly 90 K. At this temperature one sees primarily the phonon emission process in the indirect transition from the valence band to the lowest conduction band.¹ In this case the quantity $\alpha h\nu$ is proportional to $(h\nu - E_g)^2$, where E_g is the experimental energy gap and $h\nu$ is the photon energy. The energy E_g is related to the fundamental gap E_0 by $E_g = E_0 + \hbar\omega$, where $\hbar\omega$ is the average phonon energy emitted in the direct transition.¹ In this letter we will always consider the gap to be the measured quantity E_g as obtained by fitting $\alpha h\nu$ with this quadratic expression.

A typical set of data on four samples covering the range of Ge concentrations studied is shown in Fig. 1. The dominant threshold feature is marked for each sample. Note that the threshold energy decreases monotonically with increasing Ge content, as expected. The weak, low-energy feature

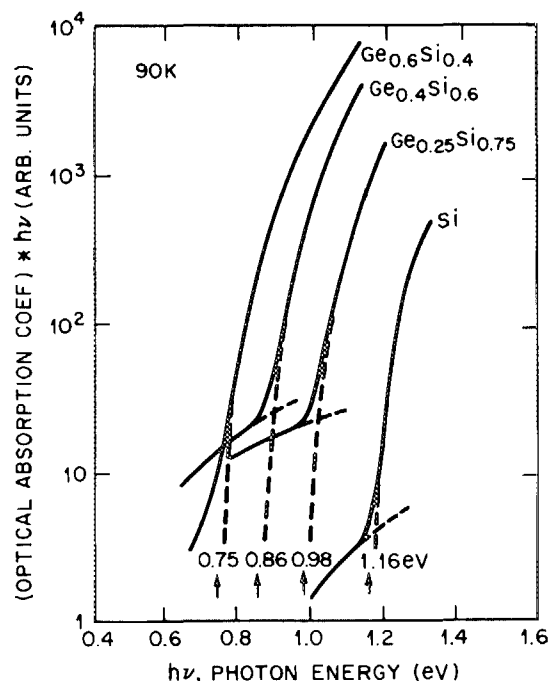


FIG. 1. Normalized photocurrent spectra for four samples. The energies indicate the lowest quadratic threshold for each sample.

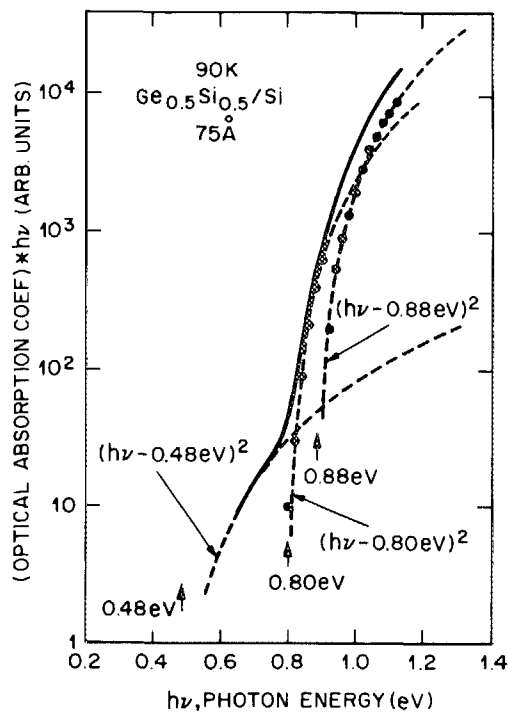


FIG. 2. Fitting procedure for a typical sample. Note the thresholds at 0.8 and 0.88 eV which are believed to be due to the strain splitting of the GeSi valence band.

seen in some of the samples is most likely due to defects. This defect signal is currently being studied and will be the subject of a subsequent publication.

A closer examination of the data indicates that the absorption edge can be best fit by the sum of two expressions of the form $(h\nu - E_g)^2$ with a slightly different value of E_g for each. This type of fitting procedure for a typical sample ($x = 0.5$) is shown in Fig. 2. One first fits the lowest energy defect feature (0.48 eV in Fig. 2) with this quadratic shape and subtracts it from the data. As this is continued to the higher energy thresholds in Fig. 2, one can see two well-defined quadratic absorption edges at 0.80 and 0.88 eV in spite of the fact that the raw data do not show an obvious feature for the higher of these two thresholds. We know that this kind of two-component absorption edge is not an artifact of the measurement, however, because it does not occur in pure Si *p-i-n* diodes or Schottky barriers. As we shall see, the energy separation between the two components of the Ge-Si absorption edge is exactly that predicted for the strain splitting of the alloy valence band. Therefore, we shall interpret the two thresholds as illustrated in Fig. 2 and seen in all samples for $x > 0.25$ as a splitting of the valence band of the coherently strained Ge-Si alloy.

A summary of the threshold data for the six samples studied is shown in Fig. 3. Note the two thresholds seen for the samples having Ge content $\geq 40\%$. Also shown in this figure are the calculated absorption thresholds for coherently strained layers using the method of Ref. 8 and the data on bulk Ge-Si alloys from the literature¹ measured near this same temperature.

Before we discuss the remarkable agreement with the theory of Ref. 8, we should point out one further part of our analysis which gives us increased confidence in our fitting procedure. Namely, we must correct for the quantum shifts

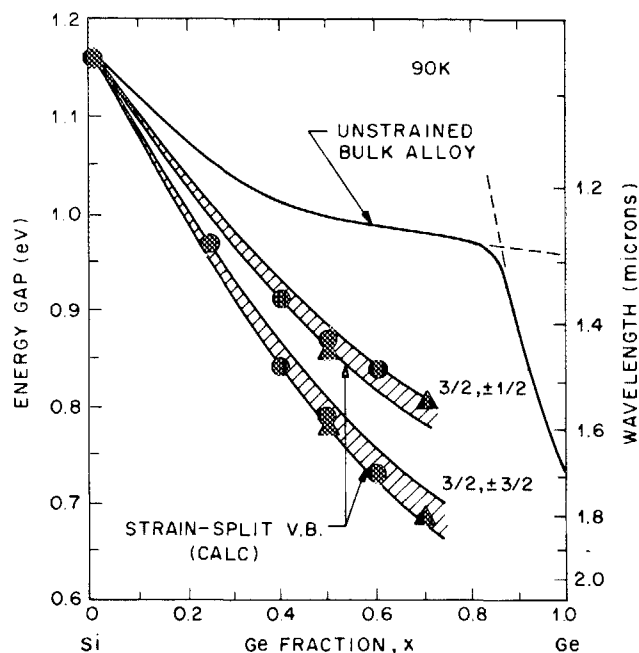


FIG. 3. Summary of energy-gap values at 90 K after correcting for quantum well shifts (circles = 75 Å wells; triangles = 33 Å wells). The double points at the same values of x correspond to a splitting of the valence band as shown in Fig. 2. The unstrained bulk alloy data are from Ref. 1. The calculations showing the strain-split valence band are indicated by the cross-hatched bands.

associated with the fact that the Ge-Si layers are thin enough (33–75 Å) so that quantum confinement effects are measurable. The actual absorption edge is shifted from E_g by the distance of the quantum well state above the bottom of the well. From magnetotransport measurements on Ge-Si/Si heterostructures we know that most of the band-gap discontinuity is in the valence band.² Thus we can attribute the band-gap difference between the alloy and the Si cladding layers to a quantum well roughly 400 meV deep for two-dimensional holes. The effective mass of two-dimensional holes in Ge-Si has been measured to be 0.3 m_0 . Therefore, the quantum well shift for a 75-Å well is 12 meV. This is only slightly larger than the estimated uncertainty in our measurement. However, for a sample with a 33-Å well the correction is 65 meV. As seen in Fig. 3 the two samples at $x = 0.5$ agree quite well after this shift is taken into account, even though one sample had a 75-Å well (12 meV shift) and the other had a 33-Å well (65 meV shift).

The calculated transition energies in Fig. 3 were obtained by combining x-ray diffraction data³ for the in-plane and normal strain components in alloy layers with measured values of the deformation potential constants for Si⁹ and Ge,¹⁰ so as to evaluate the strain matrix elements in the phenomenological strain Hamiltonian of Kleiner and Roth.¹¹ Uniaxial splittings of the sixfold degenerate valence-band edge were calculated using the 6×6 Hamiltonian of Hasegawa,¹² which includes strain-induced couplings between the $J = 3/2$ (upper valence band) and the spin-orbit split-off $J = 1/2$ band. The Si layers in the SLS are known to be unstrained for commensurate growth on Si substrates.¹³

The uniaxial strain components cause the normally fourfold degenerate $J = 3/2$ upper valence band to split into a set of two doublets. For growth on $\langle 001 \rangle$ Si, the alloy

layers experience a simple tetragonal distortion.³ In such a case, the strain operators couple only those states of $J = 3/2$ and $J = 1/2$ which have the same magnetic quantum number $\pm M_J$, i.e., $\pm M_J$ remains a good quantum number.⁹ This means that the valence-band states may be represented by (J, M_J) descriptors, as in Fig. 3. Similarly, the uniaxial strain components cause the sixfold degenerate (Si-like) conduction band of the alloy layers to split into a doublet and a fourfold degenerate set of states. The doublet is associated with the two minima along $\langle 001 \rangle$ whereas the fourfold degenerate set is associated with the four valleys normal to $\langle 001 \rangle$ and are of lowest energy in the present case. Hydrostatic deformation potential constants were obtained from Paul and Warschauer.¹⁴ An almost step-function-like behavior of the hydrostatic deformation potential is observed, changing abruptly from $+1.5$ eV for alloys having Si-like conduction-band structure to -4.5 eV for alloys having Ge-like conduction-band structure. Note then that in the calculated curves of Fig. 3 we have assumed a constant hydrostatic deformation potential of $+1.5$ eV. These results differ slightly, therefore, from those of Ref. 8; however, we believe the present values for the hydrostatic deformation potentials are more reliable.

In summary, we have used photocurrent spectroscopy to measure the optical absorption spectra of coherently strained layers of $\text{Ge}_x\text{Si}_{1-x}$ grown on Si by MBE strained-layer epitaxy. The photocurrent measurements on p - i - n diode structures at 90 K give an indirect absorption edge which can be best fit by two components with slightly different threshold energies. We see a dramatic lowering of the band gap relative to that of an unstrained bulk Ge-Si alloy. At $x = 0.6$ the gap is lower than that of pure Ge. Our results for $0 < x < 0.7$ are in remarkably good agreement with recent calculations of the effects of misfit strain on the band edges of

coherently strained Ge-Si/Si heterostructures. Not only do we observe the dramatic lowering of the band gap, which was predicted by elastic continuum theory, but we also see the predicted strain splitting of the valence band. Moving the absorption of Si-based structures into the range of $1.3\text{-}\mu\text{m}$ lightwave communications systems has obvious implications for photodetectors in this wavelength range. This ability to lower the gap with the inherent misfit strain will make it possible to achieve $1.3\text{-}\mu\text{m}$ detectors with lower Ge content and better crystal perfection than is possible with pure Ge detectors grown on Ge-Si mismatched layers.

We would like to thank V. Narayanamurti and A. Y. Cho for continued encouragement during the course of this work. We would also like to thank K. W. Wecht and A. Savage for valuable technical assistance.

¹R. Braunstein, A. R. Moore, and F. Herman, *Phys. Rev.* **109**, 695 (1958).

²R. People, J. C. Bean, D. V. Lang, A. M. Sergent, H. L. Stormer, K. W. Wecht, R. T. Lynch, and K. Baldwin, *Appl. Phys. Lett.* **45**, 1231 (1984).

³J. C. Bean, L. C. Feldman, A. T. Fiory, S. Nakahara, and I. K. Robinson, *J. Vac. Sci. Technol. A* **2**, 436 (1984).

⁴J. C. Bean, in *Proceedings of the 1st International Symposium on Silicon Molecular Beam Epitaxy*, edited by J. C. Bean (Electrochemical Society, Pennington, NJ, 1985), p. 337.

⁵H. Jorke and H. J. Herzog, in *Proceedings of the 1st International Symposium on Silicon Molecular Beam Epitaxy*, edited by J. C. Bean (Electrochemical Society, Pennington, NJ, 1985), p. 352.

⁶J. W. Matthews and A. E. Blakeslee, *J. Cryst. Growth* **27**, 118 (1974); **29**, 273 (1975); **32**, 265 (1976).

⁷G. C. Osbourn, *J. Appl. Phys.* **53**, 1586 (1982); P. L. Gourley and R. M. Biefeld, *J. Vac. Sci. Technol. B* **1**, 383 (1983).

⁸R. People, *Phys. Rev. B* **32**, 1405 (1985).

⁹J. C. Hensel and G. Feher, *Phys. Rev.* **129**, 1041 (1963).

¹⁰J. C. Hensel and K. Suzuki, *Phys. Rev. B* **9**, 4219 (1974).

¹¹W. H. Kleiner and L. M. Roth, *Phys. Rev. Lett.* **2**, 334 (1959).

¹²H. Hasegawa, *Phys. Rev.* **129**, 1029 (1963).

¹³F. Cerdeira, A. Pinczuk, J. C. Bean, B. Batlogg, and B. A. Wilson, *Appl. Phys. Lett.* **45**, 1138 (1984).

¹⁴W. Paul and D. M. Warschauer, *J. Phys. Chem. Solids* **6**, 6 (1958).